Spin susceptibility and NMR spectra of small jellium spheres

By J. P. Bucher and J. J. van der Klink

Institut de Physique Expérimentale, Ecole Polytechnique Fédérale de Lausanne, CH-1015 *Lausanne, Switzerland*

Abstract. The simple standard jellium with spherical boundary conditions is used to calculate magnetic properties. Jahn–Teller distortions away from spherical symmetry are treated in an approximate way, considering only the effect on spin multiplicity. In this approximation, the susceptibility of all open-shell particles (those with a number of electrons different from the 'magic numbers') increases with decreasing temperature. The resulting NMR line shape of an assembly of particles shows size effects (from the non uniform spin density inside the particles) and temperature effects (from the susceptibility). Our model, which goes over to a Kubo model for a statistically uniform density of states (no degeneracy), always shows an increasing susceptibility at low temperature. A few rough qualitative comparisons with available experimental data are made.

I. Introduction

Despite considerable theoretical work in the field of magnetic properties of metallic clusters, very little is known about the relation between a measured NMR line and the local magnetic information contained in it.

Local Knight shift calculations (muon and impurity shifts) have been developed to an advanced stage in bulk solids. Most of the theoretical work has been based on the jellium approximation where the metal is described by the homogeneous electron gas. These calculations were done either by adopting the charge density functional formalism [1] or the spin density functional formalism [2]. The last formalism was extended to the so-called spherical solid model which in a rough way takes into account the lattice potential [3]. By including core polarization effects, jellium models also seem to give a good description of nuclear Knight shifts in simple metals, in agreement with experimental results [4]. Because of the rotational symmetry encountered in treating impurities in the jellium approximation, spherical cluster models have also been employed in describing impurities in infinite solids [5].

In the present work we are interested specifically in cluster calculations. The situation in small particles is different in that we are not faced with the calculation of the nuclear Knight shift for a privileged nucleus, say an impurity at the center of the particle, but rather with the calculation of many different Knight shifts at

different sites in the particle. In this respect the case of small particles is very peculiar because of the very broad Knight shift distribution encountered. Due to the boundaries, the electron probability density varies from site to site inside the particle and the Knight shift has values above as well as below the bulk value. In addition, the finite size of the particle leads to temperature variations in the NMR spectrum through the temperature dependence of the total magnetization.

Actually, magnetic properties of small metallic particles, especially temperature effects, have been mostly studied by means of statistical models [6] (the set of one electron levels is considered as a statistical object). This approach has led to the prediction that, at low temperature, the susceptibility depends on the parity of the number of electrons per particle.

The purpose of this work is not to do a comprehensive calculation of Knight shifts in small particles but rather to show with extremely simple model how both 'local' (probability density) and 'non-local' (susceptibility) effects contribute to the NMR line. To our knowledge, no simultaneous treatment of both effects has been given so far.

A summary account of this work has been published previously [7].

II. Electronic properties in systems with discrete levels

Consider a small system ('small particle'), containing N non-interacting electrons confined in a volume V. We suppose that the set of one-electron eigenvalues $\{E_k\}$, their degeneracies $\{d_k\}$, as well as their corresponding eigenfunctions $\{\psi_k\}$ are known. For sake of simplicity, we will use the grand canonical rather than the more appropriate canonical ensemble. The predictions concerning the behaviour of the susceptibility are qualitatively similar for the two ensembles [8], differing mainly in the prediction of the 'threshold temperature' below which effects become visible. This point will be discussed in more detail in section V. Then, at any finite temperature, the probability of occupation of a state of energy E is given by the Fermi–Dirac distribution function

$$f(E) = [1 + \exp(\beta(E - \zeta))]^{-1} \tag{1}$$

where $\beta = 1/kT$ and ζ is the chemical potential. The latter quantity is implicitly defined through the average total number of conduction electrons in the system

$$N = \sum_k d_k f(E_k), \tag{2}$$

where d_k is the degeneracy including spin.

The Fermi level is the low temperature limit of the chemical potential:

$$E_F = \lim_{T \to 0} \zeta(N, T). \tag{3}$$

The zero-field electron spin-only susceptibility is

$$\chi(T) = \frac{-\mu_0 \mu_B^2}{V} \sum_k d_k \left(\frac{\partial f}{\partial E}\right)\bigg|_k. \tag{4}$$

The Knight shift originates from the conduction electron spin polarization, which gives rise to a local field at the site of the probe nucleus. In the case of a simple metal, this local field arises only through the Fermi contact term. In the small field limit (first order perturbation), the general expression for the Knight shift of a nucleus at site $\mathbf{r}$ becomes

$$K(\mathbf{r}) = -\tfrac{2}{3}\mu_0\mu_B^2 \sum_k \left(\frac{\partial f}{\partial E}\right)\bigg|_k \sum_{p=1}^{d_k} |\psi_{k,p}(\mathbf{r})|^2, \tag{5}$$

which is valid as long as $\mu_B B_0 \ll kT$ and the right-hand side is evaluated at zero field.

In bulk metals with a simple lattice, all nuclear sites $\mathbf{r}$ are related by translation symmetry, and K is independent of $\mathbf{r}$. This is not necessarily true in a small particle, and a range of K-values will result. Similarly, Knight shift measurements in dilute alloys are shown to give local spin susceptibility informations for the nearest and next-nearest neighbour of an impurity [9].

For the infinite solid, the relations corresponding to equations (2), (4) and (5) follow immediately by introducing the density of states (DOS) at the chemical potential ζ and temperature T:

$$D(\zeta, T) = -\sum_k d_k\left(\frac{\partial f}{\partial E}\right)\bigg|_k. \tag{6}$$

The low temperature limit of equation (6) is compatible with the usual definition:

$$D(E) = \sum_k d_k\delta(E_k - E). \tag{7}$$

In a free electron gas with parabolic DOS

$$D(\zeta, T) = \frac{V}{2\pi^2}\left(\frac{2m_e}{\hbar^2}\right)^{3/2} E_F^{1/2} = \frac{3N}{2E_F}. \tag{8}$$

Therefore, the susceptibility remains constant until very low temperatures. This is the usual Pauli susceptibility; m_e is the mass of the electron.

Figure 1 shows in a schematic way why the situation in the bulk, where equation (8) is valid, is different from that in a small particle where equation (6) applies. The DOS (equation (6)) in a small particle in general is temperature dependent. Such a temperature dependence of χ is not unique to systems with discrete energy levels: in bulk transition metals the spin susceptibility depends on the temperature, due to a sharp structure of the electronic DOS of the d-band. To find the low-temperature behaviour of equation (6), two cases have to be considered.

For particles with all energy levels completely filled up to level k_0, the low-temperature chemical potential is

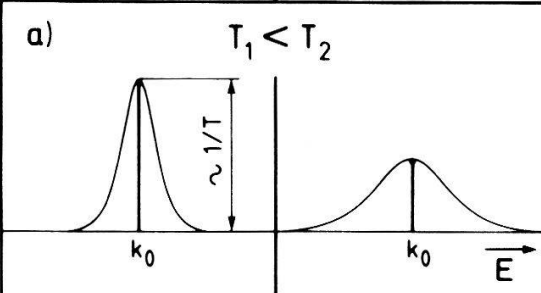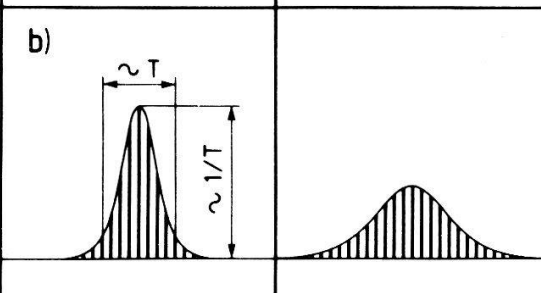$$2\zeta = E_{k_0+1} + E_{k_0} - kT \log\frac{d_{k_0+1}}{d_{k_0}} \tag{9}$$

	$-\sum_k d_k\, \delta(E_k - E)\, \dfrac{\partial f}{\partial E}$		$-\sum_k d_k\, \dfrac{\partial f}{\partial E}\Big|_k$	$X(T)$
	T_1	T_2		
Particle with $N_{k_0} = d_{k_0}/2$	a) $T_1 < T_2$ [peak at k_0, $\sim 1/T$]	[broader peak at k_0, axis E]	$-d_{k_0} \dfrac{\partial f}{\partial E}\Big|_{k_0}$	$\sim \dfrac{1}{T}$
Infinite solid	b) [narrow peak, width $\sim T$, height $\sim 1/T$]	[broad peak]	$-\displaystyle\int_0^\infty D(E)\, \dfrac{\partial f}{\partial E}\, dE$ $= D(E_F^{bulk})$	independent of T

Figure 1

Schematic representation of the sum term in equation (4). (a) Particles in which the sum in equation (4) limits to the only term k_0. The susceptibility is proportional to the maximum amplitude of the derivative of the Fermi function. This leads to a purely Curie like variation of the susceptibility at low temperature. (b) When the particle size is growing, and as soon as the level spacing between two adjacent levels becomes very small with regard to kT, it is possible to define an average DOS. The sum term in (4), more and more tends to be replaced by an expression like (8).

and E_F is halfway between E_{k_0} and E_{k_0+1}. The density of states (and the susceptibility) tends to zero with decreasing temperature as

$$D(\zeta, T) \cong \frac{2}{kT}(d_{k_0} d_{k_0+1})^{1/2} \exp\left[\frac{E_{k_0} - E_{k_0+1}}{2kT}\right]. \tag{10}$$

If the highest occupied energy level E_{k_0} (in the ground state) is only partially filled (with a number of electrons N_{k_0} less than d_{k_0}), ζ varies at low temperatures as:

$$2\zeta = 2E_{k_0} + 2kT[\log N_{k_0} - \log(d_{k_0} - N_{k_0})] \tag{11}$$

and $E_F = E_{k_0}$. Note that for an exactly half-filled level, the linear term in T disappears. The DOS becomes:

$$D(\zeta, T) \cong \frac{1}{kT} N_{k_0}(1 - N_{k_0}/d_{k_0}) \tag{12}$$

and the susceptibility shows Curie behaviour.

III. The free electron gas with spherical boundary conditions

Theoretical descriptions of the magnetic properties of metallic particles [6] usually start from the assumption that the average spacing δ of electron energy levels around the Fermi energy E_F is a smooth function of the number N of electrons in the particle:

$$\delta = 4E_F^{\text{bulk}}/3N. \tag{13}$$

The success [10] of the spherical model [11] in explaining the size dependence of cluster abundances, and in describing their polarizabilities, seems to indicate however that there might be a considerable variation in electron level structure. Therefore, we propose here an extremely simplified way to take account of the electronic structure of small particles in the description of susceptibilities and Knight shift. We will consider the standard jellium (smeared out nuclear charge and Hartree–Fock approximation for the electron-electron interaction) and we neglect relativistic effects. The solutions of the one electron Schroedinger equation are:

$$\psi_{n,l,m}(r,\,\theta,\,\phi) = \sqrt{\frac{2}{R}} \; \frac{j_l(k_{n,l}r)}{rj_{l+1}(X_{n,l})} \, Y_{l,m}(\theta,\,\phi), \tag{14}$$

$$E_{n,l} = \frac{h^2 k_{n,l}^2}{2m_e}; \qquad k_{n,l} = \frac{X_{n,l}}{R}, \tag{15}$$

where the set of eigenfunctions $\{\psi_{n,l,m}\}$ and the set of eigenvalues $\{E_{n,l}\}$ are selected by the boundary conditions: $j_l(X_{n,l}) = 0$ (Dirichlet boundary conditions); j_l is the spherical Bessel function of order l and $X_{n,l}$ is the nth zero of j_l, $Y_{l,m}(\theta,\,\phi)$ are the usual spherical harmonics, m is the projection of l on the z-axis. The radius of the particle is given by $R = N^{1/3} r_s$ where N is the number of valence electrons and r_s is the usual electron density parameter. The important point is that each level $(n,\,l)$ has a degeneracy of $2(2l + 1)$. The formulae from section II apply, with substitution of k by $(n,\,l)$ and d_k by $2(2l + 1)$.

Partly filled shells have considerable orbital degeneracy, so that the resulting ground state particle shape and spin multiplicity are determined by competition between the Jahn–Teller effect and Hund's rule. At least for alkali metal clusters, this results probably always in Jahn–Teller distortions, and low-spin (singlet or doublet) ground states [12, 13]. As a result, the closed-shell clusters are spherical in shape; those with $(4q - 2)$ or $(4q - 1)$ (q integer) electrons outside closed shells are ellipsoidal and remaining ones spheroidal; 'even' particles (with an even number of electrons) have spin singlets as ground state, 'odd' particles (with an odd number of electrons) have spin doublets. We will assume that the distortions from spherical symmetry in spheroidal and ellipsoidal particles have a perturbational effect on the corresponding spherical single-particle energy levels $E_{n,l}$, and that the resulting spread in energy $\Delta_{n,l}$ of non-degenerate energy levels is small compared to the average difference $(\Delta E)_{n,l}$ between subsequent $E_{n,l}$. In that case there should be a range of temperature such that $\Delta_{n,l} < k_B T < (\Delta E)_{n,l}$ where a
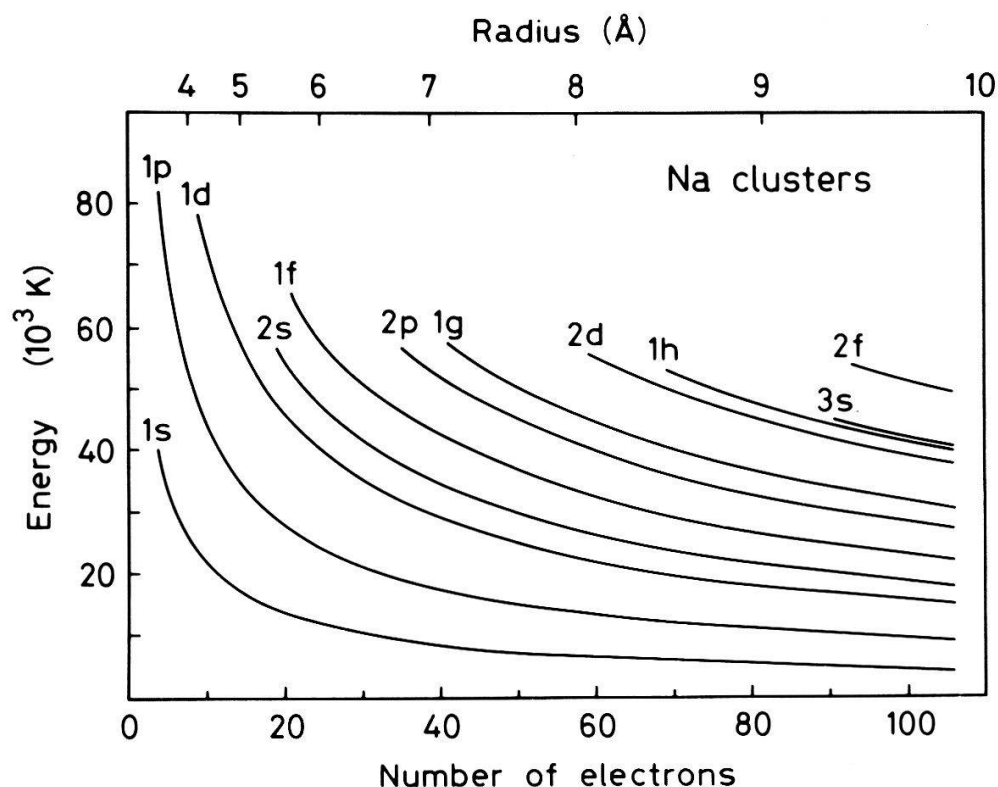
Figure 2
One electron eigenvalues for sodium particles as a function of the number N of atoms in a cluster.

considerable simplification of numerical computation can be made by assuming all levels originating from the same $E_{n,l}$ equally populated. Although the range of applicability of this 'effective spherical' approximation is unclear *a priori*, it should provide at least qualitative information on the behaviour of the non degenerate system at not too low temperatures. We will make a few more remarks on this approximation afterwards.

Most of our calculations were done for sodium ($r_s = 3.93$), which is believed to be the best replica of the ideal jellium. In Fig. 2, we have reported the one electron ground state eigenvalues $E_{n,l}$ for sodium clusters, calculated with equation (15), as a function of the cluster size N. It shows the typical energy jumps of the last occupied level which precisely corresponds to sizes with $N = 2$, 8, 18, 20, 34, etc ... filling a shell. Figure 3 shows $\zeta - E_F^{\text{bulk}}$ for two different temperatures as a function of the cluster size. The higher temperature was only chosen in order to show a difference on the scale of the drawing. The two curves cross for half filled shells, according to equation (11). Interesting is also the fact that the chemical potential of small particles is always higher than that of the bulk, in agreement with classical thermodynamic results.

A study of the eigenfunction aspect of the solution (14), tells us that the more important the orbital quantum number l is, the bigger is the probability to find an electron near the surface. Since the highest orbital numbers l still occupied (obtained for $n = 1$) are those near the Fermi energy and have the highest degeneracy, we expect a surface contribution which can be important in the final expression of the Knight shift.
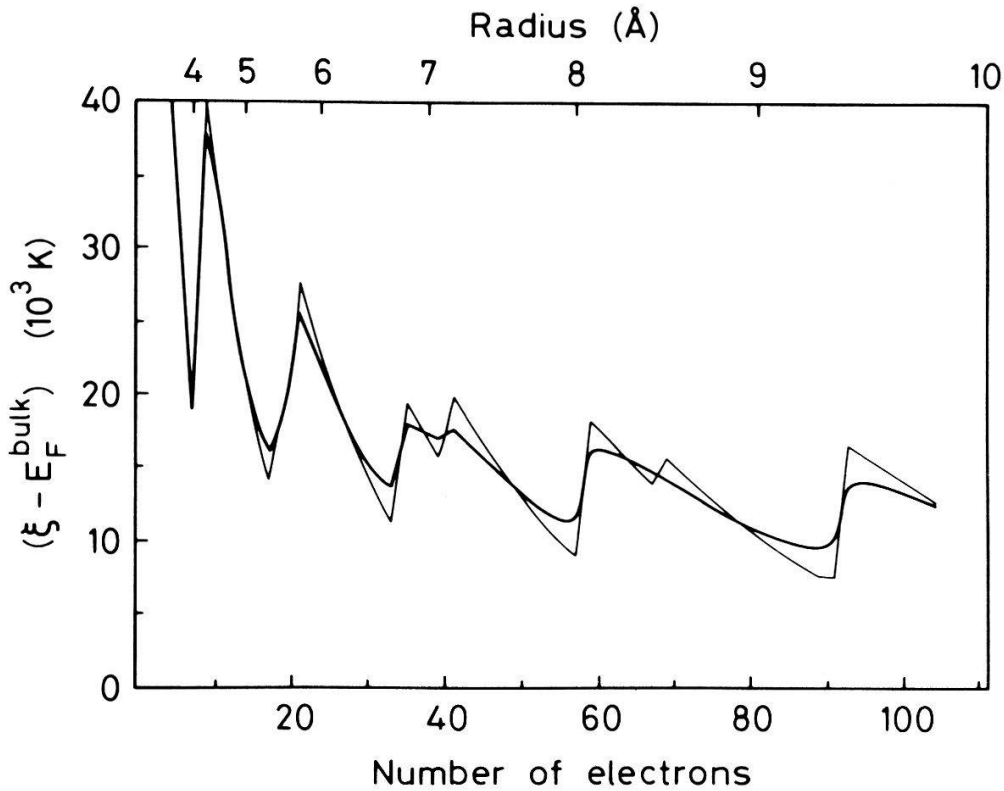
Figure 3
ζ-E_F^{bulk} as a function of the particle size for $T = 1000$ K (thick solid line) and for $T = 0$ K (thin solid line), for sodium particles.

For consistency it is of course required that upon increasing their size, the DOS of our jellium spheres tends to the DOS of the bulk jellium. This was shown to be the case, according to the early work of H. Weil[1]). In the Appendix, we present an approach to this problem based on a WKB approximation. Here we give only a simple estimate of the variation of energy level spacing, that can be obtained from equation (15) by analyzing the variation of each energy level as a function of N. Assuming $E_{n,l}(N')$ to be the energy level (n, l) for the particle of number N' of conduction electrons, then, from Eq. (15), the energy $E_{n,l}(N)$ for any N, is given by

$$E_{n,l}(N) = \left(\frac{N'}{N}\right)^{2/3} E_{n,l}(N');$$ (16)

we conclude that the separation between adjacent levels also diminishes as $N^{-2/3}$. All 'metallic' properties e.g. electron conduction, magnetic susceptibility, can be derived from the idea that there are unoccupied levels arbitrary close (i.e. within an interval $\ll kT$) to ζ (or to E_F at sufficiently low temperatures). Clearly this can only be true for an 'infinite' system and a 'small particle' will not always be metallic.

---

[1]) H. Weil [14] proved that the assymptotically leading term of the mode density is only proportional to the volume V of the domain, regardless of its shape. See also Ref. 15 and Refs. therein.

Consider the susceptibility of the spherical jellium. Even if we neglect the diamagnetic contribution [16], the spherical symmetry still leads to an orbital and a spin paramagnetic contribution to the susceptibility. However, in a real particle, the orbital momentum will be quenched by the translational motion of the electron through the lattice. For this reason, we limit our considerations to the spin contribution, as given by equations (4) and (5). Of particular interest is the effect of the derivative of Fermi function. This function acts as a 'window'. Increasing the number of levels inside the window has a smoothing effect on the size-dependence of the susceptibility. For a given temperature, we can increase the number of levels inside the window by augmenting the particle size, or for a given particle, we can increase the number of levels inside the window by augmenting the width of the window (the temperature). A somewhat heuristic view is to say that filling more and more the window (high temperatures or big particles) makes the particle to 'forget' its shell structure.

In the simple spherical jellium (where one disregards the discreteness of the lattice), the discontinuity at the boundary is a source of spin-orbit coupling. In simple j-coupling the eigenfunction solutions then are of the form [17]:

$$\Psi_{\nu,\lambda}(r, \theta, \phi) = R_\nu(r)\Gamma_{\nu,\lambda}(\theta, \phi). \tag{17}$$

Here the $\Gamma_{\nu,\lambda}$ are not eigenfunctions of the Zeeman interaction; it can be shown that $\Gamma_{\nu,\lambda}$ is coupled by the Zeeman interaction to $\Gamma_{-(\nu+1),\lambda}$ that differs in one unit of j, but has identical l and m_j. But since the $R_\nu(r)$ for different index ν are orthogonal, the total eigenfunctions $\Psi_{\nu,\lambda}$ are not mixed. As a consequence, although the 'effective' spin is changed by the spin-orbit coupling, no second order spin-Zeeman effects, as proposed by Sone [18], exist in this model.

Whereas a particle of given size has one unique value of the susceptibility (at a given temperature), its NMR spectrum will contain a number of lines at different values of the Knight shift. From equation (14) and (5), we obtain:

$$K(r) = -\tfrac{2}{3}\mu_0\mu_B^2 \sum_{\{n,l\}} \frac{2l+1}{\pi R} \left(\frac{\partial f}{\partial E}\right)\bigg|_{(n,l)} \left[\frac{j_l(k_{n,l}r)}{rj_{l+1}(X_{n,l})}\right]^2. \tag{18}$$

When the thermal energy is small compared to the degenerated level spacing, the mean contribution to the magnetization only comes from the last occupied level (n_0, l_0). In that case, equation (18) reduces to

$$K(r) = -\tfrac{2}{3}\mu_0\mu_B^2 \frac{2l_0+1}{\pi R} \left(\frac{\partial f}{\partial E}\right)\bigg|_{(n_0,l_0)} \left[\frac{j_{l_0}(k_{n_0,l_0}r)}{rj_{l_0+1}(X_{n_0,l_0})}\right]^2; \qquad 0 < N_0 < 2(2l_0+1) \tag{19}$$

and

$$N_0 = 2(2l_0 + 1)f(E_{n_0,l_0}, \zeta_0), \tag{20}$$

N_0 being the amount of electrons occupying the last level. Expression (19) brings out two factors. The first one is essentially non-local, it is roughly the magnetization of the particle as a whole and represents the eigenvalue aspect while the second factor containing the square of the wave function is of local nature and represents the eigenfunction aspect.
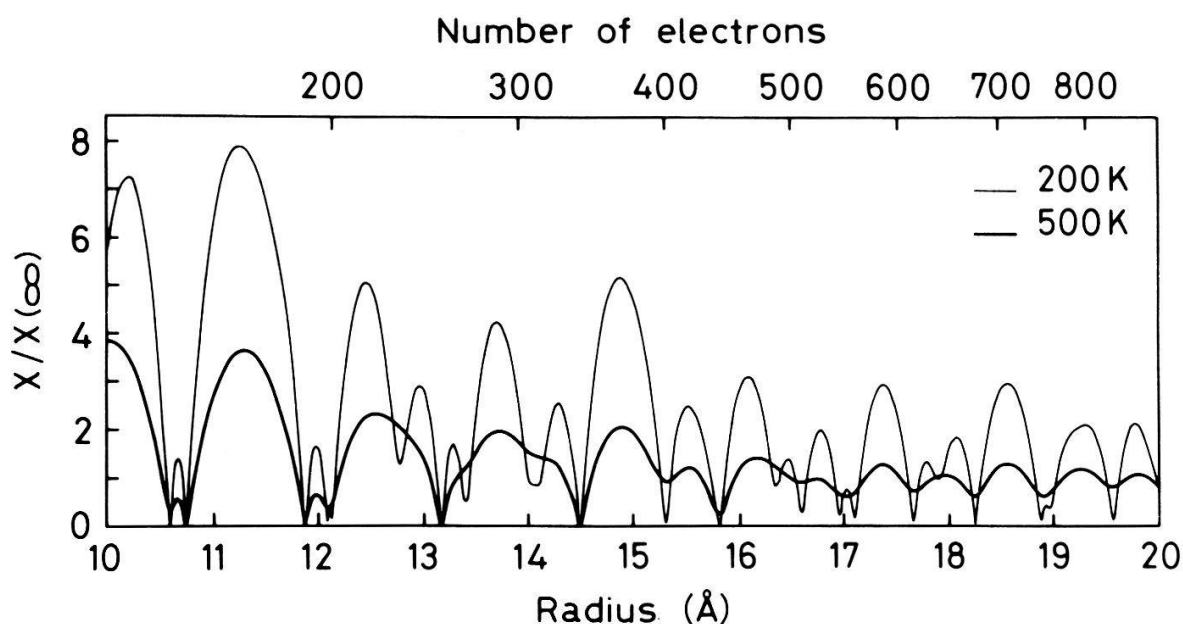
Number of electrons

Figure 4
Spin susceptibility of 'effectively spherical" jellium particles as a function of the particle size at two different temperatures. The electron density parameter $r_s = 3.93$ a.u., as appropriate for Na. Units are the susceptibility for the corresponding bulk jellium: $\chi(\infty) = 8.2 \times 10^{-6}$ (SI units).

IV. Results

In Fig. 4, we have calculated the susceptibility as given by equation (4) as a function of the particle size for two different temperatures. From this figure, the smoothing-out effect of the shell structure, both for bigger particle sizes and for higher temperatures becomes clear. The dimensionless magnetic susceptibility tends towards the infinite jellium value for Na: 8.2×10^{-6} (SI units). Particles with completely filled shells have (close to) zero susceptibility; the maxima occur for half-filled shells. In a sample with a distribution of sizes, the Curie behaviour will dominate because most particles have an unfilled shell.

NMR spectra were calculated according to equation (18) for samples with distributions of size represented in Fig. 5 and for various temperatures. Where calculations were done as a function of the particle size (see Fig. 6), the size distributions of Fig. 5 are normalized so that the total amount of reasonating nuclei remains constant. As the mean particle size in Fig. 6 increases, the amount of particles with a filled shell (contributing to zero susceptibility), diminishes with regard to those with an incomplete shell. This explains that finally the peak at $K = 0$ tends to disappear for big particles. For distribution 3 the center of gravity of the NMR line (roughly determined by the susceptibility) is already close to that of the bulk, but the considerable width of the line reflects the large number of non-equivalent sites in the particles.

On the other hand Fig. 7 represents NMR line shape calculations in the low temperature limit (50 K, 150 K) where only the last occupied level has to be considered, see equation (19). The short vertical lines indicate the corresponding
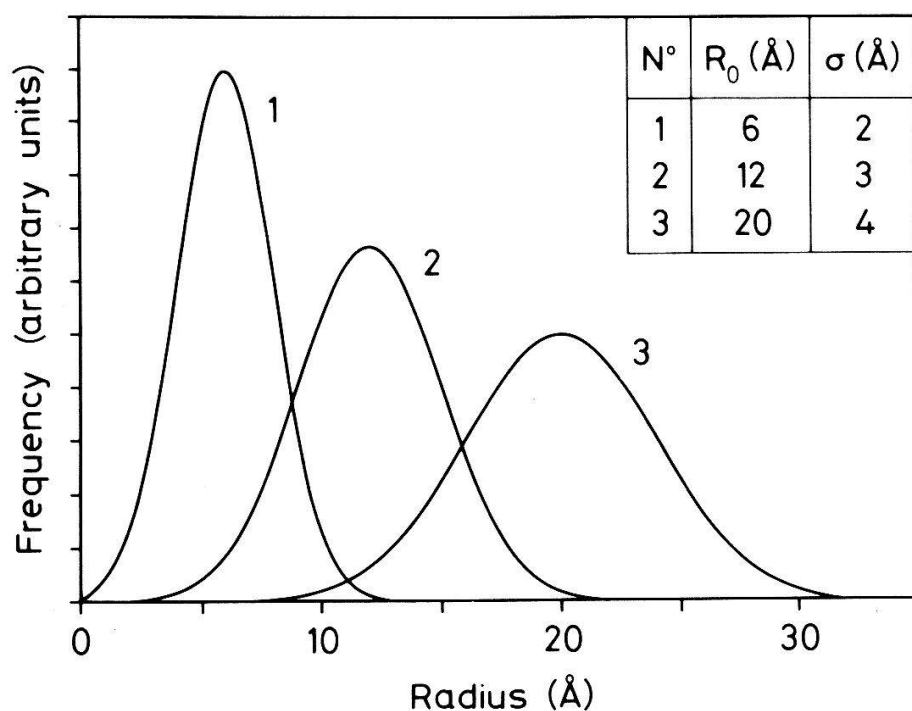
Figure 5

Normal size distributions used in our calculations: R_0 is the most probable particle radius and σ is the width of the distribution given both in Å.
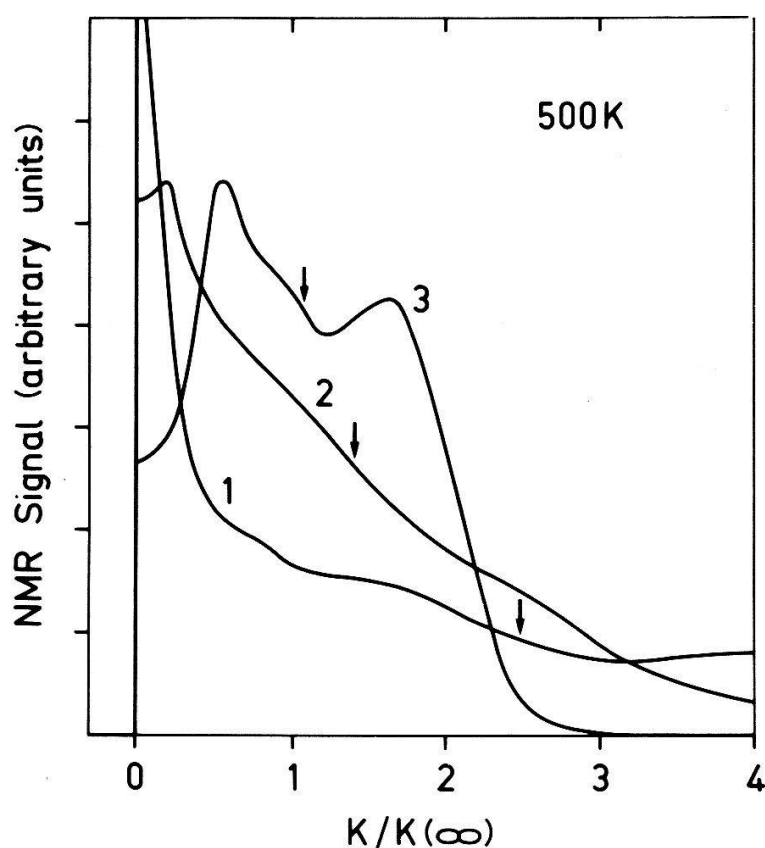
Figure 6

Convergence of the NMR line towards that of the bulk for increasing particle size. The numbers correspond to the size distributions in Fig. 5. The horizontal scale is in units of $K(\infty)$, the (site- and temperature-dependent) Knight-shift of the bulk jellium. The NMR frequency increases to the right. For distribution Nr. 3, up to 2700 particles were considered in the calculation. Vertical arrows indicate the corresponding average Knight shifts.
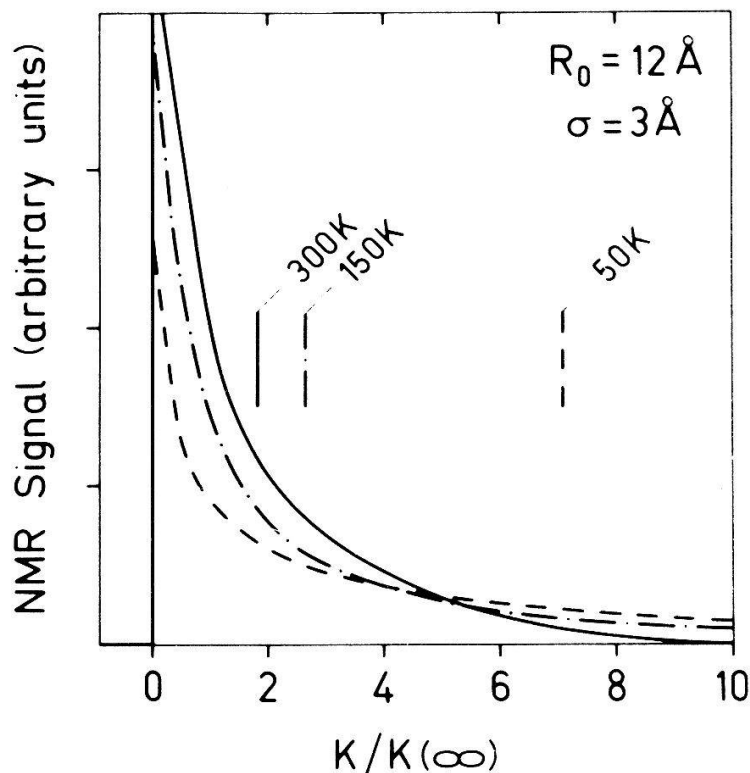
Figure 7
Calculated NMR spectra for a normal distribution of 1500 sodium particles (Nr. 2 of Fig. 5) at three different temperatures. The average Knight shifts are indicated by the short vertical lines. Spectra are normalized to the same area.

average Knight shifts which could be the informations obtained from conduction electron spin resonance (CESR) measurements on these particles (CESR only gives an average susceptibility information).

The most remarkable feature of the lines in Fig. 7 is the strong temperature dependence. In fact, as the temperature diminishes the line extends more and more towards higher Knight shifts. Finally, since the area under the line has to remain constant, (conservation of the number of resonating centers) the line will dilute totally. This behaviour can easily be understood by going back to the expression for the susceptibility as a function of T given by equation (4), since the wave function Ψ is supposed to be independent of the temperature. Of course, the discussion applied to equation (4) (see Fig. 1) remains valid.

V. Discussion

The model shows how the smallness of the particles affects their magnetic properties. The NMR lines show 'local' effects due to the non uniform spin density inside the particles as well as 'non local' temperature effects from the susceptibility.

The 'local' effect results in an asymmetrical line shape, with a width of the order of the bulk Knight shift. This effect has also been discussed by other

authors [19, 20, 21]; it is neglected in models using statistical distributions of levels (Kubo-type theories) [6].The size-dependence of the susceptibility is an additional cause of line broadening in a sample of non-uniform particles.

The susceptibility effects shows up as a strong temperature-dependence of the center of gravity of the NMR signal (Fig. 7) that, due to the low-intensity wings in the low field region, would experimentally probably show up only as a line close to zero shift with a width (FWHM) less than the bulk Knight shift; the line width being smaller (and therefore its apparent center closer to $K = 0$) for lower temperatures. This temperature variation of the susceptibility was not considered in Refs. [19, 20, 21], and is described in a different way in Kubo-type theories. We will not review these theories here (for a review see Ref. 6), but only point out some differences with the present model.

In the Kubo model, the wave function aspect is left out and only energy levels are taken into account. The central assumption concerning the energy levels are that all degeneracies are lifted by surface irregularities and that their energies are randomly distributed around the Fermi level, with their spacing Λ obeying a given statistics $P(\Lambda) \sim \Lambda^{\gamma} \exp\left[-(\Lambda/\delta)^2\right]$ ($\gamma = 1, 2 \ldots$ depending on the statistical ensemble). This situation is described in our equations by $d_k = 2$ independent of k, and $N_{k_0} = 1$ in equation (12). Then from equations (10) and (12) we have:

$$\chi_{\text{even}} \cong \frac{\mu_0 \mu_B^2}{V} \frac{4}{kT} \exp\left[-(\Lambda/2kT)\right], \tag{21}$$

$$\chi_{\text{odd}} \cong \frac{\mu_0 \mu_B^2}{V} \frac{1}{2kT}. \tag{22}$$

The susceptibility will exhibit the Curie behaviour for the odd case (particles with an odd number of electrons) while the susceptibility in the even case (even number of electrons) is exponentially attenuated. The fact that in statistical models one has to average over a distribution $P(\Lambda)$, does not change the situation much. Then $\langle \chi_{\text{even}} \rangle$ varies with T^{γ} rather than exponentially while $\langle \chi_{\text{odd}} \rangle$ still varies as T^{-1} [7]. The corresponding canonical ensemble results [8] vary with δ/kT in the same way. Therefore, we expect no important qualitative differences between canonical and grand canonical averaging (for quantitative differences, compare Fig. 2 of Ref. 8). Whatever $P(\Lambda)$ is, the criterion to observe a quantum size effect or not, remains that the thermal energy kT be smaller than the average level spacing δ:

$$\delta = \int \Lambda P(\Lambda) \, d\Lambda = \frac{4 E_F^{\text{bulk}}}{3N}. \tag{23}$$

In Fig. 8, we have reported $\delta/2$ and $1/D(\zeta, T)$ at 150 K for our model, (equation (6)). At this temperature, most of jellium particles with $N < 160$ are still metallic ($D^{-1}(\zeta, T) < kT$) while Kubo particles are not.

It will be clear from the discussion that the essential difference between the present and the statistical models lies in the assumptions concerning the
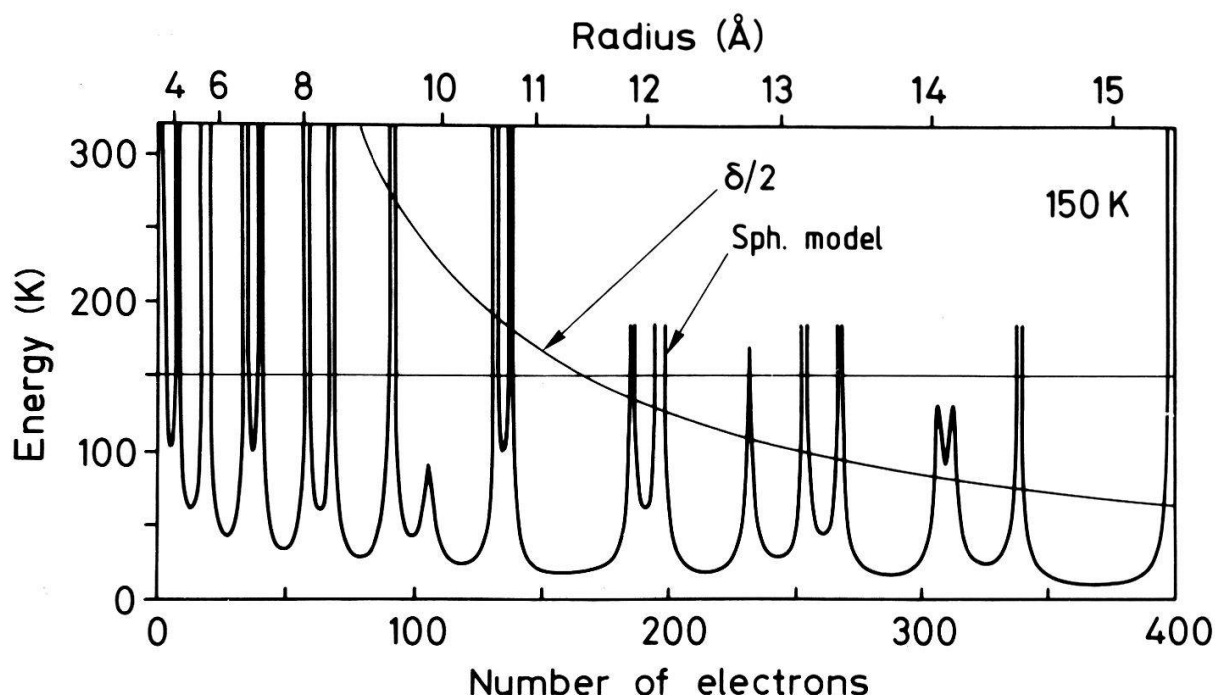
Figure 8
$\delta/2 = 2E_F^{bulk}/3N$ and $1/D(\zeta, T)$ for the spherical model as a function of particle size for sodium at 150 K (horizontal line).

geometrical symmetry and the quasi degeneracy of the energy levels that follows from it. The differences between spherical and ellipsoidal geometries, or even the differences between a free-electron model (as in the present paper) and a tight-binding approach (the opposite case)[2]) probably play a minor role in comparison. So, it is tempting to conclude that the result of our model could be fairly general. Small irregularities would have the effect of partially lifting degeneracies, but in small particles, we remain with degeneracies due to the dominant symmetry.

A remarkable result of this 'effective spherical' model is that the neglect of the splittings $\Delta_{n,l}$ largely suppresses the distinction between 'odd' and 'even' particles (leaving only 'open shell' and 'closed shell' particles). As a consequence, predictions for mono- and divalent metals are very similar, as shown in Fig. 9 for sodium and magnesium particles with the same distribution. The neglect of the splittings might be not too crude an approximation for most temperatures used in our calculations, but there will of course always be a lower limit to its validity. As an example, consider a half-filled outer shell with a large value of l, and let the result of Jahn–Teller and exchange couplings be a splitting into $(2l + 1)$ equidistant levels, spaced Δ apart. If $\Delta \ll kT$ and $(2l + 1)\Delta \gg kT$ (which of course implies rather large particles), the average spacing around the Fermi level

---

[2])   The local DOS in our problem being defined as $D(E, \mathbf{r}) = \sum_{k,p} \delta(E_k - E) |\Psi_{k,p}(\mathbf{r})|^2$, the general formulation developed in section II can be directly applied to the LCAO problem by replacing $\psi_{k,p}(\mathbf{r})$ by the coefficients $a_{\mathbf{r},p}(E_k)$ of the atomic orbitals of degeneracy p which have to be considered.
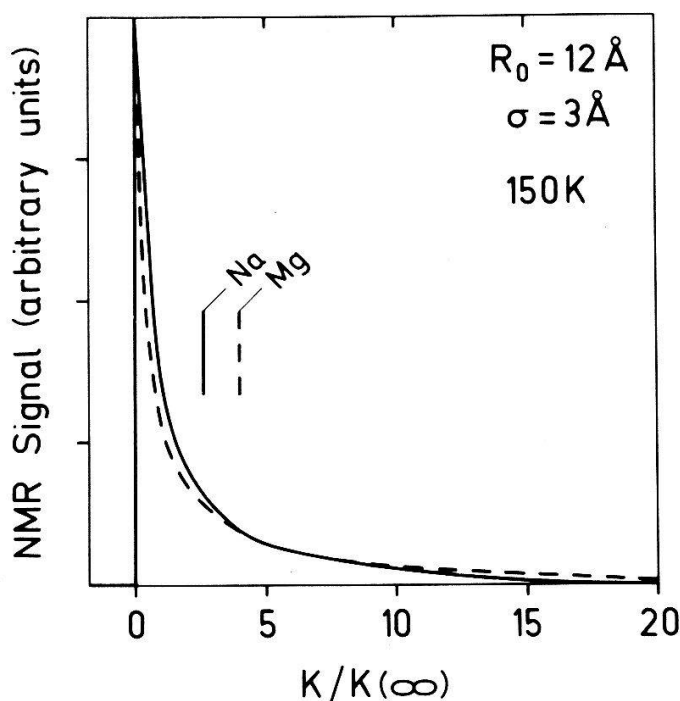
Figure 9
NMR spectra with parameters corresponding to Na ($r_s = 3.93$ a.u., N odd and even) and to Mg ($r_s = 2.66$ a.u.; N even only) for the same size distribution (Nr. 2 of Fig. 5). Spectra are normalized to the same area.

will be Δ, much smaller than δ, and the resulting susceptibility will be more Pauli- then Curie-like. Similarly particles with an even number of electrons in an unfilled outer shell will have a nonzero, Pauli-like, susceptibility. Without more detailed knowledge about how the initial $E_{n,l}$ degeneracies are lifted it is difficult to discuss this more specifically: it might for example happen that a particle size distribution in the jellium model has an effect similar to that of Kubo's Poisson distribution [22] (where 'accidental' degeneracies have a nonzero probability) for a level spacing at constant size.

Experimentally, there is some support for this latter idea in ESR data on small Mg particles [23], but the totality of results for this metal in the literature shows little consistency. Size-dependent NMR spectra as in Fig. 6 have been consistently found for platinum particles by two groups [24, 25] (for an exception see Ref. 20); but neither of them found a remarkable temperature dependence between 4 and 77 K. The observation of one single line arising from Li platelets [26] in neutron irradiated LiF (instead of one line from 'even' and one line from 'odd' particles; see however Ref. 27) at fairly high temperature (300 K) follows from the present model without invoking excessive line broadening due to the size distribution. The NMR experiments of Yee and Knight on copper [28] were performed at very low temperatures, where the validity of our approximations is doubtful, still the decrease of linewidth and of Knight shift [28] below 8 K for a sample with a relatively poor signal-to-noise ratio is consistent with our discussion of Fig. 7. Again, conflicting reports from other laboratories exist.

For large level spacings δ the nuclear spin-lattice relaxation time T_1 should become very long (compared to the value in the bulk metal); this effect has not been reported so far, which is compatible with conditions of large l and small Δ, similar to those described in a previous paragraph.

Although the experimental situation remains unclear, in that few consistent effects have been reported by different laboratories, it seems that existing data on magnetic effects in small particles of normal metals can be at least as well understood from the well-defined but irregular level structures of the shell model, as from the usual models using statistical distributions of equally-spaced levels (and some effects [29] are hard to understand in either class of models).

Acknowledgments

Appendix: WKB approximate eigensolutions for the spherical model

Sometimes, it is very useful to have at one's disposal an analytical expression for $j_l(x)$ and its zeroes. Usually in the asymptotic domain ($l^2 \ll x$), $j_l(x)$ is approximated by:

$$j_l(x) = \sin\left(x - \frac{l\pi}{2}\right). \tag{A1}$$

The corresponding eigenvalues for our problem are given by:

$$X_{n,l} = \pi\left(n + \frac{l}{2}\right). \tag{A2}$$

However, in most applications (for instance in order to see the convergence of the DOS towards the bulk jellium), we need an expression for j_l and $X_{n,l}$ which is valid in a wider range than the asymptotic one. One way to do this, is to use a WKB approximation (see for instance Ref. 30). The Schroedinger radial equation for our problem is:

$$\chi_l'' + q^2\chi_l = 0, \tag{A3}$$

with

$$q^2 = k^2 - U_l(r). \tag{A4}$$

For short wavelengths, $U_l(r) = l(l+1)/r^2$ may be considered constant for several

wavelengths about r, then:

$$\chi \cong \frac{1}{q^{1/2}} \sin \left(\int q(r) \, dr \right);$$

(A5)

$$\int q(r) \, dr = (x^2 - L^2)^{1/2} + L \arcsin \frac{L}{|x|} + C,$$

(A6)

where $L^2 = l(l + 1)$ and $x = kr$. The validity of the approximation is restricted to [30]:

$$L^2/x^3 \ll \left(1 - \frac{L^2}{x^2} \right)^{3/2}.$$

(A7)

Therefore the approximation is valid for $l \ll x$. Putting (A6) into (A5) we obtain:

$$\chi \cong \frac{1}{q^{1/2}} \sin \left\{ x \left(1 - \frac{L^2}{x^2} \right)^{1/2} + L \arcsin \frac{L}{x} + C \right\}.$$

(A8)

Equation (A8) must tend to the asymptotic form (A1) when $x \to \infty$; this fixes the integration constant $C = -l\pi/2$. Setting $L \cong l$, the argument of the sin in (A8) becomes:

$$x \left(1 - \frac{l^2}{2x^2} \right) + \frac{l^2}{x} - \frac{l\pi}{2} + 0 \left(\frac{l}{x} \right)$$

(A9)

it follows

$$j_l(x) \cong \left\{ \left(x - \frac{l\pi}{2} \right) + \frac{l^2}{2x} \right\}.$$

(A10)

This WKB solution is the continuation of the asymptotic form (A1), therefore we call it preasymptotic.

By equating the argument of the sin in equation (A10) to $n\pi$, we obtain the solutions of the eigenvalue problem as:

$$2X_{n,l} = \left(n\pi + \frac{l\pi}{2} \right) + \left[\left(n\pi + \frac{l\pi}{2} \right)^2 - 2l^2 \right]^{1/2}.$$

(A11)

$X_{n,l}$ is related to the energy eigenvalues by equation (15). Our new expression for $X_{n,l}$ is valid in a wider range than the old asymptotic one. We use it in order to show that the DOS of our small jellium particles tends to the DOS of the bulk free electron model for big particles.

By setting the maximum value of $X_{n,l}$ in a given particle to be $X = X_{n_{max},0}$ ($n_{max} = n(l = 0)$), the total number of states N_T up to X is given by:

$$N_T = \int_{n=1}^{n_{max}} \int_0^{l(n)} 2(2l + 1) \, dl \, dn,$$

(A12)

where the upper boundaries are given by:

$$2l(n) = X\pi - [X^2\pi^2 - 8(X^2 - n\pi X)]^{1/2}$$

(A13)

and

$$n_{max} = X/\pi. \tag{A14}$$

The integration leads to

$$N_T = 0.1341X^3 + 0(X^2). \tag{A15}$$

Using equation (A15) and the relation between X and E (equation (15)), we get:

$$\frac{dN_T}{dE} = \frac{3}{2} 0.1341\left(\frac{2m_e}{\hbar^2}\right)XR^2 + 0(1). \tag{A16}$$

Finally, the DOS at E_F can be written in the following form:

$$D(E_F) = \frac{V}{2\pi^2} \alpha\left(\frac{2m_e}{\hbar^2}\right)^{3/2} E_F^{1/2}. \tag{A17}$$

Our preasymptotic approximation leads to $\alpha = 0.948$, while for the free electron case $\alpha = 1$. With the simple asymptotic approximation, the result should have been $\alpha = 0.608$. Thus, that we find a factor α different from one is only due to our difficulty in counting states. However, we approach the value of one by increasing the accuracy of our analytical approximation.

REFERENCES

[1] P. Jena and K. S. Singwi, Phys. Rev. 17, 3518 (1978).
[2] K. G. Petzinger and R. Munjal, Phys. Rev. 15, 1560 (1977).
[3] M. Manninen and R. M. Nieminen, J. Phys. F9, 1933 (1979).
[4] E. Zaremba and D. Zobin, Phys. Rev. Lett. 44, 175 (1980).
[5] A. Hinterman and M. Manninen, Phys. Rev. 27, 7262 (1983).
[6] J. A. A. J. Perenboom, P. Wyder and F. Meier, Physics Reports 78, 173 (1981), see also H.-P. Baltes and E. Simànek, in Aerosol Microphysics II, Topics in Current Physics, Vol. 29, (Springer, Berlin, 1982).
[7] J.-P. Bucher and J. J. van der Klink, Solid State Commun. 65, 27 (1988).
[8] R. Denton, B. Muehlschlegel and D. J. Scalapino, Phys. Rev. B7, 3589 (1973).
[9] I. D. Weismann and W. D. Knight, Phys. Rev. 169, 373 (1968).
[10] W. D. Knight, W. A. de Heer, W. A. Saunders, Z. Phys. D.3, 109 (1986) and refs. therein.
[11] J. L. Martins, R. Car and J. Buttet, Surf. Sci. 101, 265 (1981).
[12] J. L. Martins, J. Buttet and R. Car, Phys. Rev. B31, 1804 (1985).
[13] S. N. Khanna, Proc. Int. Symposium on Physics and Chemistry of Small Clusters, Virginia (1987).
[14] H. Weyl, Rend. Circ. Mat. Pal. 39, 1 (1915).
[15] H.-P. Baltes and E. R. Hilf, Spectra of Finite Systems, (Bibliographisches Institut AG, Zürich, 1976).
[16] W. Mercouroff, La Surface de Fermi des Métaux, (Masson, Paris, 1967).
[17] M. E. Rose, Elementary Theory of Angular Momentum, (John Wiley and Sons, New York, 1957).
[18] J. Sone, J. Phys. Soc. Japan 42, 1457 (1977).
[19] R. J. Charles and W. A. Harrison, Phys. Rev. Lett. 11, 75 (1963).
[20] I. Yu and W. P. Halperin, J. Low Temp. Phys. 45, 189 (1981).
[21] C. D. Makowka, C. P. Slichter and J. H. Sinfelt, Phys. Rev. 31, 5663 (1985).
[22] R. Kubo, A Kawabata and S. Kobayashi, Annu. Rev. Mat. Sci. 14, 49 (1984) and Refs. therein.
[23] J. L. Millet and J. P. Borel, Surf. Sci. 106, 403 (1981).

[24] H. E. RHODES, P. K. WANG, H. T. STOKES, C. P. SLICHTER and J. H. SINFELT, Phys. Rev. *B26*, 3559 (1982).

[25] J. J. VAN DER KLINK, J. BUTTET and M. GRAETZEL, Phys. Rev. *B29*, 6352 (1984).

[26] J. CHARVOLIN, C. FROIDEVAUX, C. TAUPIN and J. M. WINTER, Solid State Commun. *4*, 357 (1966).

[27] J. CHARVOLIN, J. P. COHEN-ADDAD and C. FROIDEVAUX, Solid State Commun. *5*, 357 (1967).

[28] W. D. KNIGHT, J. Vac. Sci. Technol. *10*, 705 (1973).

[29] K. KIMURA and S. BANDOW, Phys. Rev. Lett. *58*, 1359 (1987).

[30] P. M. MORSE and H. FESHBACH, *Methods of Theoretical Physics*, (McGraw-Hill, New York, 1956) p. 1092.